Magnetic Flux Noise in dc SQUIDs: Temperature and Geometry Dependence

S. M. Anton,[1] J. S. Birenbaum,[1] S. R. O'Kelley,[1] V. Bolkhovsky,[2] D. A. Braje,[2] G. Fitch,[2] M. Neeley,[2] G. C. Hilton,[3] H.-M. Cho,[3] K. D. Irwin,[3] F. C. Wellstood,[4] W. D. Oliver,[2] A. Shnirman,[5] and John Clarke[1]

[1]*Department of Physics, University of California, Berkeley, California 94720-7300, USA*
[2]*MIT Lincoln Laboratory, 244 Wood Street, Lexington, Massachusetts 02420, USA*
[3]*National Institute of Standards and Technology, Boulder, Colorado 80309-044, USA*
[4]*Department of Physics, University of Maryland, College Park, Maryland 20742, USA*
[5]*Institut für Theorie der Kondensierten Materie, Karlsruhe Institute of Technology, D-76128 Karlsruhe, Germany*

(Received 17 October 2012; published 5 April 2013)

The spectral density $S_\Phi(f) = A^2/(f/1\ \mathrm{Hz})^\alpha$ of magnetic flux noise in ten dc superconducting quantum interference devices (SQUIDs) with systematically varied geometries shows that α increases as the temperature is lowered; in so doing, each spectrum pivots about a nearly constant frequency. The mean-square flux noise, inferred by integrating the power spectra, grows rapidly with temperature and at a given temperature is approximately independent of the outer dimension of a given SQUID. These results are incompatible with a model based on the random reversal of independent, surface spins.

DOI: 10.1103/PhysRevLett.110.147002 PACS numbers: 85.25.Dq, 05.40.−a, 85.25.Am

Flicker ($1/f$) noise at low frequencies f is observed in all solid state devices. In particular, $1/f$ noise in superconducting quantum bits (qubits) [1] is the leading cause of decoherence (loss of phase coherence) as the state of the qubit evolves. The resulting reduction in the pure dephasing time τ_ϕ limits the fidelity of qubit readout and inhibits scaling up to multiple qubit circuits. In some cases, the origin of the noise is reasonably well understood. For example, in charge-sensitive devices such as charge qubits [2] $1/f$ noise arises from the hopping of electrons between nearby traps that induce fluctuating charges on the qubit. In the case of Josephson tunnel junctions—which are constituents of flux [3] and phase [4] qubits and superconducting quantum interference devices (SQUIDs) [5]—$1/f$ noise in the critical current (maximum supercurrent) arises from the trapping of electrons in the barrier and their subsequent release [6]. The mechanism for magnetic flux $1/f$ noise, however, with a power spectrum $S_\Phi(f) = A^2/(f/1\ \mathrm{Hz})^\alpha$, has remained poorly understood. Here, Φ is flux and $\alpha \lesssim 1$. Flux noise is a major source of intrinsic dephasing [7] in superconducting flux [8–12] and phase qubits [7,13,14] and in the quantronium [15]; it also generates low-frequency noise in SQUIDs [16–18].

It has been proposed that flux noise originates from the random reversal of spins at the interfaces between the superconductor and its substrate and surface oxide layer [19–21]. Models that assume independent spins with a magnetic moment μ_B (the Bohr magneton) predict an areal spin density of $5 \times 10^{17}\ \mathrm{m}^{-2}$. The same value is found from measurements of paramagnetism in SQUIDs [22] and Au rings [23]. Noise correlation measurements on flux qubits are consistent with the surface spin model [11,12].

A crucial question is whether the independent-spin model describes the flux noise dynamics correctly or if spin-spin interactions are significant. Sendelbach *et al.* [24] inferred the existence of clusters from measurements of inductance fluctuations in SQUIDs, suggesting a non-negligible spin-spin interaction. The independent-spin model was used in an analytical calculation of the mean-square value of the flux noise $\langle\Phi^2\rangle$ as a function of loop geometry [13,20]. Measurements of decoherence in flux qubits [10] were in agreement with the predicted scaling while measurements of decoherence in phase qubits instead showed a scaling with loop inductance [14].

In this Letter we report flux noise measurements as a function of temperature for ten dc SQUIDs with systematically varied geometries. We find that both $S_\Phi(1\ \mathrm{Hz})$ and the slope α vary systematically with temperature. Remarkably, for a given SQUID $S_\Phi(f)$ pivots about a nearly fixed frequency as the temperature is changed. Values of $\langle\Phi^2\rangle$ inferred from our measurements of $S_\Phi(f)$ deviate markedly from the predicted scaling with loop geometry. Furthermore, although there is no evident temperature dependence in the prediction of $\langle\Phi^2\rangle$ over the range of temperatures investigated, pivoting causes the inferred values of $\langle\Phi^2\rangle$ to vary over several orders of magnitude as we change the temperature. We are unable to reconcile our data with the independent-spin model.

We measured $S_\Phi(f)$ in a total of 20 dc SQUIDs, connected in series in sets of 5 on four chips, fabricated on oxidized Si wafers using a trilayer Nb-AlOx-Nb junction technology. Two chips were made at MIT-LL and two at NIST. Since the two chips from each institution showed very similar results, we present data on only one from each, labeled I (LL) and II (NIST). The SQUIDs were patterned in a square geometry with outer widths $2R$ and loop line widths W listed in Table I, along with their estimated loop inductances. Each junction was resistively shunted to eliminate hysteresis on its current-voltage characteristic.

TABLE I. Dimensions and inductances of SQUIDs I and II.

	R (μm)	W (μm)	R/W	L (pH)
I.1	12	0.5	24	80
I.2	6	0.5	12	33
I.3	3	0.5	6	12
I.4	1.5	0.5	3	4
I.5	1.5	0.5	3	4
II.1	265	240	1.1	120
II.2	145	120	1.2	98
II.3	85	60	1.3	92
II.4	55	30	1.8	96
II.5	40	15	2.7	106

As shown schematically in Fig. 1, the five SQUIDs on a given chip were connected in series with an off-chip compensating resistor $R_c = 0.46\ \Omega$, the input coil of a readout SQUID operated in a flux-locked loop (FLL), and a choke to suppress high-frequency currents [25]. The entire circuit was enclosed in two superconducting shields and a cryoperm shield to reduce ambient magnetic field fluctuations and the Earth's static magnetic field. The magnetic flux in the SQUIDs was established by means of a current in a common coil. To measure the flux noise in a given SQUID, we biased it at a voltage of 2.5 or 5 μV with a current I_b and canceled the quasistatic current induced in the input coil and remaining SQUIDs with a compensating current I_r in R_c. Fluctuations $\delta\Phi$ in Φ of the measured SQUID induced a current $\delta\Phi(dI/d\Phi)$ in the input coil of the readout SQUID. For all data represented here, we biased the SQUID where $dI/d\Phi$—determined by measuring the response to a small oscillating flux—was a maximum. The temperature T, measured using calibrated Ge (mixing chamber) and RuOx (sample box) resistance thermometers, was stabilized with feedback from the Ge thermometer to better than 1 part in 10^4 during data acquisition [26]. Nyquist noise from R_c yielded a temperature within $\pm 5\%$ of that of the thermometers.

We acquired a time series of the voltage fluctuations for 1 hour, computed the spectral density and converted it to

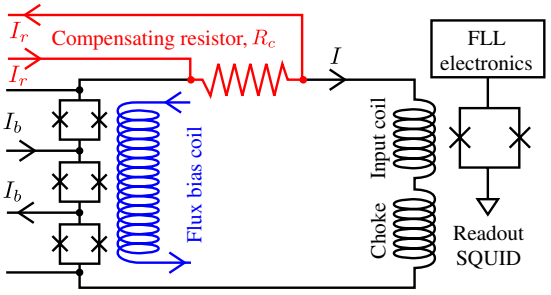

FIG. 1 (color online). Configuration of measurement system to measure flux noise in three SQUIDs. The bias current I_b enables the measurement of the middle SQUID. The static voltage across the SQUID is canceled by the current I_r applied to R_c.

$S_\Phi(f)$. We performed a least squares fit to $S_\Phi(f) = A^2/(f/1\ \mathrm{Hz})^\alpha + C^2$, representing the flux $1/f^\alpha$ noise and the white noise from the resistive shunts, to obtain A and α. To confirm that the inferred value of A^2 was independent of $dI/d\Phi$, we measured the noise at other values of Φ and $dI/d\Phi$. In addition, we made measurements at $dI/d\Phi = 0$, enabling us to determine the critical current $1/f$ noise. We verified that the power spectrum of the white noise from the resistive shunts dominated those from R_c and the readout electronics, and that, with a flux bias of $n\Phi_0$, it remained white at frequencies down to the $1/f$ knee of the readout electronics with a magnitude in reasonable agreement with theoretical predictions [27]. Here, n is an integer and $\Phi_0 \equiv h/2e$ is the superconducting flux quantum.

As representative data, in Fig. 2(a) we show raw power spectra for SQUID II.3. The spectra are $1/f$-like, with a slope that flattens at higher frequencies as the white noise from the shunt resistors becomes significant. At low frequencies ($f \lesssim 10^{-1}$ Hz) and high temperatures ($T \gtrsim 1.2$ K), fluctuations in the critical current are significant, thereby increasing the slope of the spectra [26]. Consequently, in our fits to the spectra, we disregard noise from this region.

The fitted values of A^2 and α are plotted in Fig. 3 for all five SQUIDs on both chips. We see immediately that the systematic trends with T for each chip differ between the two chips. For chip I, A^2 increases as T is lowered to 0.1 K,

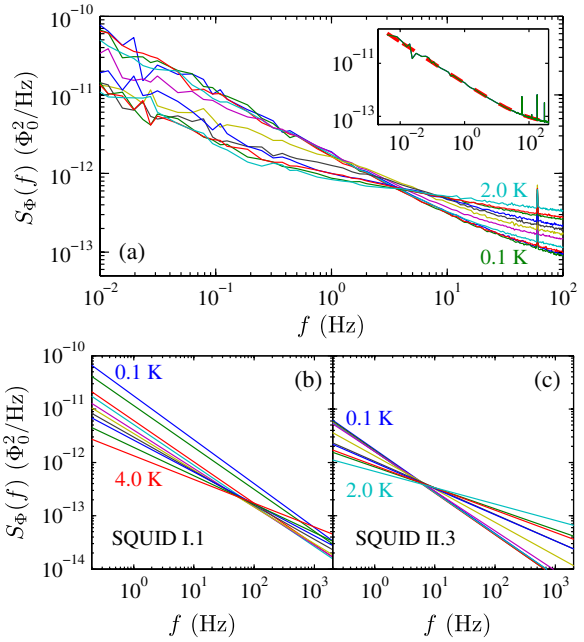

FIG. 2 (color online). Power spectra $S_\Phi(f)$. (a) As-acquired flux noise spectral densities for SQUID II.3 at 11 temperatures. Inset shows data at 0.1 K with corresponding fit to $A^2/(f/1\ \mathrm{Hz})^\alpha + C^2$ (dashed line). Fits of $S_\Phi(f)$ for (b) SQUID I.1 at 10 temperatures and (c) SQUID II.3 at 11 temperatures.

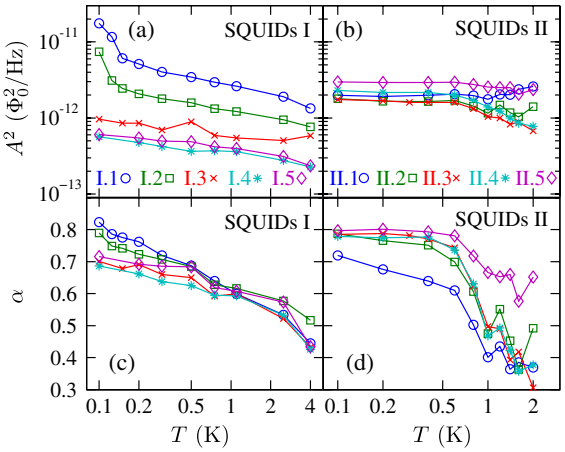

FIG. 3 (color online). Temperature dependence of $1/f$ flux noise for 10 SQUIDs. (a), (b) Fit coefficients A^2 for SQUIDs I and II vs T. (c), (d) Fit coefficients α for SQUIDs I and II vs T. Confidence in fits is $\pm 10\%$ in (a), (b); ± 0.03 ($T \leq 1.1$ K) and ± 0.05 ($T > 1.1$ K) in (c); and ± 0.03 ($T \leq 1.1$ K) and ± 0.07 ($T > 1.1$ K) in (d).

with an upturn for $T < 0.15$ K, and increases monotonically with R. In contrast, for chip II A^2 becomes independent of T for $T \lesssim 0.6$ K, a result reminiscent of the findings of Wellstood *et al.* [18]. With regard to the slope, for both chips α increases dramatically as T is lowered from 4.0 to 0.1 K. For chip I, the value of α increases with R. Similarly low values of α, 0.4–0.5 at 4 K, have been observed by other authors [17,28]. Although we have no explanation for the disparate dependencies of A^2 and α on T, we remark that for chip I W is constant at 0.5 μm while for chip II W varies from 15 to 240 μm. A conceivable explanation is that interactions between spins give rise to spatial correlations.

The progressive increase in α as T is lowered is illustrated vividly in Figs. 2(b) and 2(c), where we plot $A^2/(f/1\ \text{Hz})^\alpha$ for SQUID I.1 [Fig. 2(b)] and II.3 [Fig. 2(c)] for all T at which we obtained data. Ignoring the two highest spectra in Fig. 2(b)—corresponding to $T < 0.15$ K with upturns in the data in Fig. 3(a)—quite unexpectedly and remarkably we observe that each set of spectra pivots around an approximately constant frequency f_p: $f_p = 76 \pm 20$ Hz in Fig. 2(a) and $f_p = 6.2 \pm 0.5$ Hz in Fig. 2(b). The Supplemental Material [29] shows similar plots for all ten SQUIDs. The plots in Fig. 2 imply that, although one traditionally defines the noise magnitude as $A^2 \equiv S_\Phi(1\ \text{Hz})$, in fact A^2 is an incomplete characterization in the absence of a knowledge of α.

We next estimate the mean-square flux noise $\langle \Phi^2 \rangle$. For a circular loop of outer radius R and line width W, in the limit $R \gg W$, Bialczak *et al.* [13] showed that

$$\langle \Phi^2 \rangle \simeq \frac{2\mu_0^2}{3} \mu_B^2 \sigma \frac{R}{W} \left[\frac{\ln(2bW/\lambda^2)}{2\pi} + 0.27 \right] \qquad (1)$$

for uncorrelated spins with uniform surface density σ and magnetic moment μ_B. Here, μ_0 is the vacuum permeability, b is the film thickness, and λ is the penetration depth. For the square geometry of our devices, there is a multiplicative correction of order unity, which we neglect. Because we cannot directly measure $\langle \Phi^2 \rangle$, we use

$$\langle \Phi^2 \rangle = \int_{f_1}^{f_2} S_\Phi(f) df \qquad (2)$$

to relate $\langle \Phi^2 \rangle$ to our measurements of $S_\Phi(f)$. Here, we extrapolate $S_\Phi(f)$, which we measure typically over several decades, to f_1 and f_2. We set $f_1 = 10^{-4}$ Hz, approximately the lowest frequency to which flux noise has been measured. The value of f_2 is more difficult to estimate as it is poorly understood. Since Bylander *et al.* [30] and Slichter *et al.* [31] observed flux noise up to measurement-limited frequencies of 20 MHz and 1 GHz, respectively, we use $f_2 = 10^9$ Hz for our analysis. Separate measurements on Al SQUIDs, fabricated in exactly the same way in the same equipment as the qubits in Ref. [31], yielded average low-temperature values remarkably similar to those observed in SQUIDs I and II: $A^2 = 2.1(\mu\Phi_0)^2/\text{Hz}$ and $\alpha = 0.72$. These results suggest that details of the processing do not greatly alter the characteristics of flux noise. In particular, we expect f_2 to be comparable in SQUIDs and qubits alike.

For all ten SQUIDs, Fig. 4 shows $\langle \Phi^2_{\text{inf}} \rangle$, inferred using Eq. (2) and the data plotted in Fig. 3, vs T. For comparison, the dashed lines indicate the value of $\langle \Phi^2_{\text{calc}} \rangle$ for each SQUID calculated using Eq. (1), the values of R and W from Table I, $\sigma = 5 \times 10^{17}$ m^{-2}, $\lambda = 39$ nm, and $b = 150$ nm (I), 200 nm (II). While $\langle \Phi^2_{\text{calc}} \rangle$ is independent of T for $T \ll T_c$, the values of $\langle \Phi^2_{\text{inf}} \rangle$ increase strongly with increasing T. At the lowest T, values of $\langle \Phi^2_{\text{inf}} \rangle$ exceed those of $\langle \Phi^2_{\text{calc}} \rangle$ by 1 to 2 orders of magnitude and at the highest T by 3 to 5 orders of magnitude. Clearly, the rapid calculated increase of $\langle \Phi^2_{\text{inf}} \rangle$ with T is inevitable given the behavior in Fig. 2.

As a further test of the theory, we investigated the scaling of $S_\Phi(f)$ with SQUID dimensions to compare

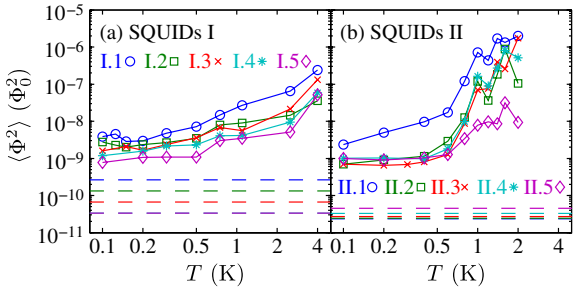

FIG. 4 (color online). Mean-square flux noise, inferred from measured power spectra using Eq. (2), vs T. (a) Chip I and (b) Chip II. Horizontal dashed lines represent the predictions of Eqs. (1) and (2) for the values of R and W listed in Table I.

with the predictions of Eq. (1). For brevity, we present results only for SQUIDs I, for which W is constant, so that $\langle\Phi^2_{\rm calc}\rangle \propto R$. Figure 5(a) shows $S_\Phi(54\ {\rm Hz})$ vs R for the four distinct geometries of SQUIDs I. Here, we chose the average value of f_p, 54 Hz, to minimize the effect of the T dependence of the spectra on the geometric scaling. To a reasonable approximation, apart from the data for SQUIDs I.1 and I.2 at the two lowest temperatures, $S_\Phi(54\ {\rm Hz})$ scales linearly with R. Figure 5(b) shows $\langle\Phi^2_{\rm inf}\rangle$ vs R for ten temperatures, which we see is approximately independent of R, increases with T, and has a magnitude substantially higher than the prediction.

We now discuss potential sources of error in $\langle\Phi^2_{\rm inf}\rangle$ that would give rise to a strong temperature dependence. A T-dependent spin density is precluded by the Curie-Law behavior of the spin paramagnetism [22,23]. We also note that, for the observed values of α, $\langle\Phi^2_{\rm inf}\rangle$ changes by less than 1% as f_1 is varied from zero to 10^{-2} Hz. With regard to f_2, one could argue that the value of $f_2 = 1$ GHz, observed at 50 mK [31], becomes lower as T increases. However, to reduce the highest-temperature value of $\langle\Phi^2_{\rm inf}\rangle$ in Fig. 5 to its lowest temperature value by lowering f_2 would require f_2 to be roughly 700 kHz for SQUIDs I and just 8 kHz for SQUIDs II. Such values of f_2 are improbably low; it is difficult to imagine a noise process that extends to 1 GHz at 0.1 K, yet to less than 1 MHz at 4 K. Regarding α, high-frequency measurements in qubits have sampled the flux noise spectrum from 0.2 to 20 MHz [30] as well as from 10^{-2} to 1 Hz, 1 to 20 MHz, and 0.7 to 1 GHz [31]. These measurements each align with a spectrum of constant α ($\alpha = 0.9$ [30] and $\alpha = 0.57$ [31]) and value of $S_\Phi(1\ {\rm Hz})$ typical of those observed in SQUIDs. These measurements suggest that, while α can vary between devices, within a single device it is frequency independent over a very wide bandwidth. Finally, errors in our fits of α will inevitably lead to errors in $\langle\Phi^2_{\rm inf}\rangle$. For instance, at low (high) temperatures decreasing α by 0.03 (0.07) increases $\langle\Phi^2_{\rm inf}\rangle$ by a factor of roughly 1.6 (4). These errors, while not negligible, cannot account for the strong temperature dependence and discrepancies of several orders of magnitude.

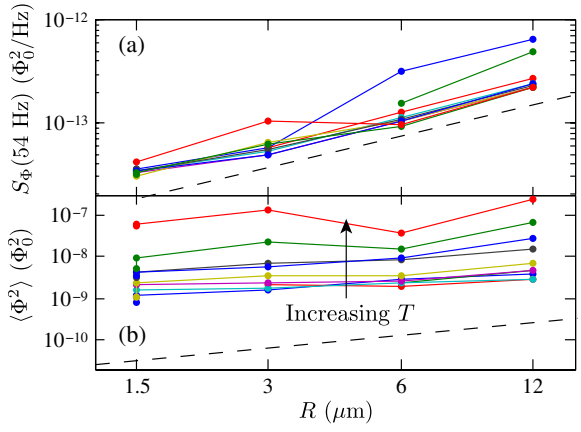

FIG. 5 (color online). Scaling of noise power with R for SQUIDs I for ten temperatures from 0.1 K to 4.0 K. (a) $S_\Phi(54\ {\rm Hz})$ vs R. Dashed line indicates scaling with R, with arbitrary magnitude. (b) $\langle\Phi^2\rangle$ vs R. Dashed line represents prediction of Eq. (1).

Given the difficulty of reconciling our data with the predictions of a model based on N single, uncorrelated spins—for which $\langle\Phi^2\rangle \propto N\mu_B^2$—we consider the possibility that the spins form clusters [24]. We assume the clusters to be uncorrelated with each other and to contain an average of Z spins producing a magnetic moment μ_c, where Z may depend on T. There are three scenarios: (i) ferromagnetic clusters with $\mu_c = Z\mu_B$ and $\langle\Phi^2\rangle \propto (N/Z)(Z\mu_B)^2 = NZ\mu_B^2$, (ii) random (glassy) clusters with $\mu_c = Z^{1/2}\mu_B$ and $\langle\Phi^2\rangle \propto (N/Z)(Z^{1/2}\mu_B)^2 = N\mu_B^2$, and (iii) antiferromagnetic clusters with $\mu_c \approx \mu_B$ and $\langle\Phi^2\rangle \propto (N/Z)\mu_B^2$. As Z grows, the rate at which a cluster reverses its magnetic moment is assumed to decrease rapidly [32]. At a given T, such a distribution of reversal rates offers a natural explanation for the 13-decade range in lifetimes required for $S_\Phi(f)$ to range from 10^{-4} to 10^9 Hz [33]. Furthermore, a plausible scenario for the spectral pivoting as T is lowered is a progressive growth in Z, reducing the number of small clusters generating noise above f_p and increasing the number of larger clusters generating noise below f_p—thereby increasing α. This simplistic picture has implications for the temperature dependence of each of the three cases. As T is lowered, $\langle\Phi^2\rangle$ increases for ferromagnetic clusters, remains constant for random clusters, and decreases for antiferromagnetic clusters.

Finally, the noise behavior must be compatible with the observed spin paramagnetism [22,23], which follows a Curie $1/T$ scaling. We note that the contribution of a cluster with magnetic moment μ_c to the linear magnetic susceptibility scales as μ_c^2/k_BT. On the other hand, once $\mu_c B > k_BT$ the susceptibility ceases to be linear in magnetic field, the magnetization of the cluster saturates and Curie scaling is violated. Consequently, since Curie behavior was observed at $T = 50$ mK and $B = 10$ mT, we find $\mu_c < 7\mu_B$. Thus, $Z < 7$ for the ferromagnetic case, $Z < 7^2$ for the random case, and Z is unrestricted for the antiferromagnetic case. We also point out that the areal single spin density of $5 \times 10^{17}\ {\rm m}^{-2}$ derived from both noise and paramagnetism experiments is unchanged for glassy clusters. Needless to say, a detailed understanding of the interactions between both the spins that form such clusters and between the clusters themselves will be required to develop a credible explanation of flux noise.

This research was funded by the Office of the Director of National Intelligence (ODNI), Intelligence Advanced Research Projects Activity (IARPA), through the Army Research Office, by the United States Government, and by the NIST Quantum Initiative.

[1] John Clarke and F. K. Wilhelm, Nature (London) **453**, 1031 (2008).

[2] Y. Nakamura, C. D. Chen, and J. S. Tsai, Phys. Rev. Lett. **79**, 2328 (1997).

[3] C. H. van der Waal, A. C. J. ter Haar, F. K. Wilhelm, R. N. Schouten, C. J. P. M. Harmans, T. P. Orlando, S. Lloyd, and J. E. Mooij, Science **290**, 773 (2000).

[4] J. M. Martinis, S. Nam, J. Aumentado, and C. Urbina, Phys. Rev. Lett. **89**, 117901 (2002).

[5] *The SQUID Handbook: Fundamentals and Technology of SQUIDs and SQUID Systems*, edited by John Clarke and A. I. Braginshi (Wiley-VCH, Weinheim, Germany, 2004), Vol. 1.

[6] D. J. Van Harlingen, T. L. Robertson, B. L. T. Plourde, P. A. Reichardt, T. A. Crane, and John Clarke, Phys. Rev. B **70**, 064517 (2004).

[7] J. M. Martinis, S. Nam, J. Aumentado, K. M. Lang, and C. Urbina, Phys. Rev. B **67**, 094510 (2003).

[8] F. Yoshihara, K. Harrabi, A. O. Niskanen, Y. Nakamura, and J. S. Tsai, Phys. Rev. Lett. **97**, 167001 (2006).

[9] K. Kakuyanagi, T. Meno, S. Saito, H. Nakano, K. Semba, H. Takayanagi, F. Deppe, and A. Shnirman, Phys. Rev. Lett. **98**, 047004 (2007).

[10] T. Lanting, A. J. Berkley, B. Bumble, P. Bunyk, A. Fung, J. Johansson, A. Kaul, A. Kleinsasser, E. Ladizinsky, F. Maibaum *et al.*, Phys. Rev. B **79**, 060509 (2009).

[11] F. Yoshihara, Y. Nakamura, and J. S. Tsai, Phys. Rev. B **81**, 132502 (2010).

[12] S. Gustavsson, J. Bylander, F. Yan, W. D. Oliver, F. Yoshihara, and Y. Nakamura, Phys. Rev. B **84**, 014525 (2011).

[13] R. Bialczak, R. McDermott, M. Ansmann, M. Hofheinz, N. Katz, E. Lucero, M. Neeley, A. O'connell, H. Wang, A. Cleland *et al.*, Phys. Rev. Lett. **99**, 187006 (2007).

[14] D. Sank, R. Barends, R. C. Bialczak, Y. Chen, J. Kelly, M. Lenander, E. Lucero, M. Mariantoni, A. Megrant, M. Neeley *et al.*, Phys. Rev. Lett. **109**, 067001 (2012).

[15] G. Ithier, E. Collin, P. Joyez, P. J. Meeson, D. Vion, D. Esteve, F. Chiarello, A. Shnirman, Y. Makhlin, J. Schriefl *et al.*, Phys. Rev. B **72**, 134519 (2005).

[16] R. H. Koch, John Clarke, W. M. Goubau, J. M. Martinis, C. M. Pegrum, and D. J. Harlingen, J. Low Temp. Phys. **51**, 207 (1983).

[17] D. Drung, J. Beyer, J. Storm, M. Peters, and T. Schurig, IEEE Trans. Appl. Supercond. **21**, 340 (2011).

[18] F. C. Wellstood, C. Urbina, and John Clarke, Appl. Phys. Lett. **50**, 772 (1987).

[19] R. H. Koch, D. P. DiVincenzo, and John Clarke, Phys. Rev. Lett. **98**, 267003 (2007).

[20] L. Faoro and L. B. Ioffe, Phys. Rev. Lett. **100**, 227005 (2008).

[21] S. K. Choi, D.-H. Lee, S. G. Louie, and John Clarke, Phys. Rev. Lett. **103**, 197001 (2009).

[22] S. Sendelbach, D. Hover, A. Kittel, M. Mück, J. M. Martinis, and R. McDermott, Phys. Rev. Lett. **100**, 227006 (2008).

[23] H. Bluhm, J. A. Bert, N. C. Koshnick, M. E. Huber, and K. A. Moler, Phys. Rev. Lett. **103**, 026805 (2009).

[24] S. Sendelbach, D. Hover, M. Mück, and R. McDermott, Phys. Rev. Lett. **103**, 117001 (2009).

[25] S. M. Anton, C. Müller, J. S. Birenbaum, S. R. O'Kelley, A. D. Fefferman, D. S. Golubev, G. C. Hilton, H.-M. Cho, K. D. Irwin, F. C. Wellstood *et al.*, Phys. Rev. B **85**, 224505 (2012).

[26] S. M. Anton, C. D. Nugroho, J. S. Birenbaum, S. R. O'Kelley, V. Orlyanchik, A. F. Dove, G. A. Olson, Z. R. Yoscovits, J. N. Eckstein, D. J. V. Harlingen *et al.*, Appl. Phys. Lett. **101**, 092601 (2012).

[27] K. K. Likharev and V. K. Semenov, Zh. Eksp. Teor. Fiz. Pis'ma Red. **15**, 625 (1972) [Sov. Phys. JETP **15**, 442 (1972)].

[28] M. Schmelz, R. Stolz, V. Zakosarenko, S. Anders, L. Fritzsch, H. Roth, and H.-G. Meyer, Physica (Amsterdam) **476C**, 77 (2012).

[29] See Supplemental Material at http://link.aps.org/supplemental/10.1103/PhysRevLett.110.147002 for similar plots for all ten SQUIDs.

[30] J. Bylander, S. Gustavsson, F. Yan, F. Yoshihara, K. Harrabi, G. Fitch, D. G. Cory, Y. Nakamura, J.-S. Tsai, and W. D. Oliver, Nat. Phys. **7**, 565 (2011).

[31] D. H. Slichter, R. Vijay, S. J. Weber, S. Boutin, M. Boissonneault, J. M. Gambetta, A. Blais, and I. Siddiqi, Phys. Rev. Lett. **109**, 153601 (2012).

[32] A. A. Khajetoorians, B. Baxevanis, C. Hübner, T. Schlenk, S. Krause, T. O. Wehling, S. Lounis, A. Lichtenstein, D. Pfannkuche, J. Wiebe *et al.*, Science **339**, 55 (2013).

[33] S. Machlup, J. Appl. Phys. **25**, 341 (1954).